9534 *Biochemistry* **2009,** *48,* 9534–9541
DOI: 10.1021/bi900770z

BIOCHEMISTRY
including biophysical chemistry & molecular biology
Article

Analysis of the Interaction of BCL9 with β-Catenin and Development of Fluorescence Polarization and Surface Plasmon Resonance Binding Assays for this Interaction†

Steven A. Kawamoto,[‡] Andrea D. Thompson,[#] Adriana Coleska,[§] Zaneta Nikolovska-Coleska,[⊥] Han Yi,[§] and Shaomeng Wang*[,‡,§,∥]

[‡]*Department of Medicinal Chemistry,* [§]*Department of Internal Medicine,* [∥]*Department of Pharmacology,* [⊥]*Department of Pathology, and* [#]*Chemical Biology Program, University of Michigan, Ann Arbor, Michigan 48109*

Received May 5, 2009; Revised Manuscript Received August 7, 2009

ABSTRACT: The transcriptional activator β-catenin is the primary mediator of the canonical Wnt signaling pathway and is frequently upregulated in many types of human cancer. Recent studies have suggested that the interaction of β-catenin and its cofactor, B-cell lymphoma 9 (BCL9), is crucial for its transcriptional activity. Targeting this interaction using small molecules will improve our understanding of the β-catenin/Wnt signaling pathway and may lead to the development of a new class of anticancer drugs. In this study, we developed a fluorescence polarization (FP)-based BCL9 binding assay. Using our initial FP assay, we performed extensive mutational analysis on four critical hydrophobic residues in the BCL9 peptide and determined the precise region in BCL9 responsible for binding to β-catenin. These results led to further optimization of our FP assay, making it amenable for high-throughput screening (HTS). We also developed and validated a complementary surface plasmon resonance (SPR)-based binding assay and showed that our synthetic BCL9-based peptides are capable of fully inhibiting the binding of β-catenin to wild-type BCL9 protein. Our studies provide not only further insight into the interaction between BCL9 and β-catenin but also quantitative and reliable biochemical binding assays for the discovery of potent and specific small-molecule inhibitors of this interaction.

The canonical Wnt signaling pathway plays a key role in various cellular processes such as regulation of cell proliferation, differentiation, and apoptosis, among others. Chronic activation of the canonical Wnt signaling pathway has been implicated in the development of a variety of human malignancies, including colorectal carcinomas, melanomas, ovarian carcinomas, and others (*1*−*3*). Mutations in the regulator genes of the Wnt signaling pathway such as the genes for adenomatous polyposis coli (APC) and Axin, as well as β-catenin itself, result in the stabilization of β-catenin and an increase in cytosolic and nuclear β-catenin protein levels. In the nucleus, β-catenin binds transcription factors T-cell factor/lymphoid enhancer factor (TCF/LEF) and additional cofactors, including B-cell lymphoma 9/B-cell lymphoma 9-like (BCL9/B9L), Parafibromin, and cAMP response element-binding protein-binding protein (CBP) (*4*−*8*) to form a supercomplex. This nuclear supercomplex causes the transcriptional activation of a number of β-catenin target genes such as c-*myc*, cyclin D1, axin-2, survivin, and multidrug resistance 1 (MDR1), which play key roles in cell proliferation, the cell cycle, apoptosis, and drug resistance (*9*−*13*). Consequently, the upregulation of β-catenin has been correlated with tumor stage and poor prognosis in a number of human cancers, and inhibition of β-catenin has been proposed as an attractive anticancer therapeutic strategy (*14*−*16*).

Since β-catenin is the primary mediator of the canonical Wnt signaling pathway, there has been intense research interest in targeting the β-catenin-containing supercomplex using small-molecule inhibitors, and a number of strategies have been pursued (*16*). One strategy is to block the interaction between β-catenin and TCF. Several small-molecule inhibitors of the β-catenin−TCF interaction have been shown to inhibit TCF reporter activity, expression of c-*myc* and cyclin D1, and the growth of colon cancer cells with constitutively activated β-catenin (*17*, *18*). Two of these compounds subsequently were shown to selectively induce apoptosis in primary acute myeloid leukemia (AML) cells (*19*). One potential limitation of such small-molecule inhibitors of the β-catenin−TCF interaction is their specificity; the TCF binding site spans much of the major groove in β-catenin and overlaps with the E-cadherin, APC, and Axin binding sites (*20*−*25*). Of particular concern is the overlap with E-cadherin, which mediates cell adhesion and is known to be a tumor suppressor involved in the transition from adenoma to carcinoma (*26*). Another strategy is to inhibit the interaction of CBP and β-catenin. A small-molecule inhibitor, ICG-001, was shown to bind selectively to CBP, inhibiting its interaction with β-catenin, causing the downregulation of survivin and cyclin D1 and inducing apoptosis in colorectal cancer cells (*27*). These studies have provided evidence that it is indeed feasible to target the nuclear β-catenin supercomplex using small-molecule inhibitors and to inhibit β-catenin activity in cancer cells.

Recent reports have suggested that the interaction of β-catenin and BCL9 represents an attractive target for designing inhibitors of β-catenin-mediated Wnt signaling (*4*−*6*, *28*−*30*). Biochemical studies have shown that BCL9 and B9L siRNAs and dominant negative gene constructs inhibit β-catenin transcriptional activity, the expression of Wnt target genes, and cancer cell migration (*28*, *31*, *32*). Furthermore, analysis of the crystal structure of

†This work was supported by the Department of Homeland Security, the University of Michigan Regents, and the American Foundation for Pharmaceutical Education.

*To whom correspondence should be addressed. E-mail: shaomeng@umich.edu. Phone: (734) 615-0362. Fax: (734) 647-9647.

 Published on Web 08/28/2009

β-catenin [Protein Data Bank (PDB) entry 2GL7] in complex with BCL9 and TCF shows that the interaction between β-catenin and BCL9 is distinct from that of other instances of β-catenin binding (*24*). This interaction is mediated by a well-defined binding groove in β-catenin and several hydrophobic and charged residues from the α-helix of BCL9. In addition, the binding is associated with a relatively high affinity whose K_d value is 0.5 μM (*24*). Hence, the BCL9 binding site in β-catenin appears to be a very attractive site for the design of potent and specific small-molecule inhibitors to block the interaction between BCL9 and β-catenin and to inhibit β-catenin-mediated signaling. To date, no small-molecule or peptide-based inhibitors of the BCL9−β-catenin interaction have been reported.

In this study, we have developed a quantitative fluorescence polarization (FP)-based binding assay using β-catenin protein and a fluorescently tagged BCL9 peptide and β-catenin protein. Using our initial FP-based competitive binding assay, we performed extensive mutational analysis on four critical hydrophobic residues in the BCL9 peptide and identified the precise region in BCL9 responsible for binding to β-catenin. These results led to further optimization of our FP assay, making it amenable for identification of nonpeptide, small-molecule inhibitors through high-throughput screening (HTS). We have also developed and validated a complementary surface plasmon resonance (SPR)-based binding assay and demonstrated that our synthetic BCL9-based peptides are capable of fully inhibiting the binding of β-catenin to the wild-type BCL9 protein with relative potencies in good agreement with those determined in the FP assay. Our studies provide not only further insights into the interaction between BCL9 and β-catenin but also quantitative and reliable biochemical binding assays for the discovery of potent and specific small-molecule inhibitors of this interaction.

EXPERIMENTAL PROCEDURES

General Procedure for Peptide Synthesis. Peptides were synthesized using standard Fmoc solid-phase peptide synthesis techniques. Briefly, Rink amide resin with either 0.2 mmol/g (for peptides ≥24 residues in length) or 0.7 mmol/g (for peptides <24 residues in length) substitution levels were used to prepare all C-terminal amide-capped peptides. Standard side chain protecting groups were used for all amino acids with the exception of N^{ε}-4-methyltrityllysine [Lys(Mtt)], which was used for coupling to fluorescein. Peptides were synthesized using an ABI 433A automated peptide synthesizer, FastMoc Chemistry, and 4−5 equiv of each amino acid.

Certain unnatural and problematic amino acids such as homoleucine (Hle) and *tert*-butylleucine (Tle) were coupled manually as follows. The resin-bound peptide was placed in a 5 mL disposable polypropylene column (Fisher Scientific), deprotected with 20% piperidine (2 × 3 mL, 15 min), and then washed with DMF (3 × 3 mL), MeOH (3 × 3 mL), and DMF (3 × 3 mL). The Fmoc-amino acid (4 equiv) was preactivated with HATU (4 equiv) and HOAt (6 equiv) in DMF (3 mL) for 10 min, treated with DIEA (6 equiv), and added to the resin. The solution was mixed by inversion for 1 h or until the resin tested negative in the Kaiser ninhydrin test (*33*). The remaining residues in the peptide were then coupled using the ABI 433A peptide synthesizer.

For fluorescein labeling, resin-bound peptides were treated with 1% TFA/DCM (5 × 1.5 mL, 15 min) to deprotect Lys(Mtt). The peptide was then treated with 5-carboxyfluorescein (5-FAM) *N*-hydroxysuccinimidyl ester (2 equiv) and DIEA (3 equiv) in dry DMF (3 mL). The reaction mixture was covered in aluminum foil and mixed by being rocked on a Clay Adams Nutator for 4 h.

Peptides were cleaved from the resin using 87.5% TFA, 5% DTT, 5% H_2O, and 2.5% TIS (3 × 2 mL, 10 min). The combined filtrates were allowed to stand at room temperature for 2 h, concentrated in vacuo, and precipitated with cold diethyl ether. The crude peptides were purified by semipreparative reverse-phase high-performance liquid chromatography (RP-HPLC) using a Waters Delta 600 HPLC system equipped with a Waters 19 mm × 150 mm Sunfire C_{18} column and a Waters 2489 UV detector. Peak fractions were concentrated and lyophilized for 16−24 h. The pure peptides were characterized by analytical RP-HPLC and electrospray ionization mass spectrometry (ESI-MS). The results are presented in Table S1 of the Supporting Information.

Recombinant Proteins. The β-catenin and BCL9 cDNAs were kind gifts from W. Xu at the University of Washington (Seattle, WA) and K. Basler of the Institut für Molekularbiologie at the Universität Zürich (Zurich, Switzerland), respectively. β-Catenin (residues 138−686) and BCL9 (residues 347−393) were cloned into a pHis-TEV vector and transformed into *Escherichia coli* BL21 DE3. Cells were cultured in LB medium with 30 μg/mL kanamycin until the OD_{600} was approximately 0.6, and then protein expression was induced with 200 μM IPTG at 20 °C overnight. Cells were lysed by sonication, and the proteins were purified by two steps of chromatography, including Ni-NTA agarose affinity chromatography and size-exclusion chromatography using an Amersham Biosciences P-920 FPLC system equipped with a Superdex 200 (for β-catenin) or Superdex 75 (for BCL9) column. β-Catenin was eluted in 30 mM bis-Tris (pH 6.5), 200 mM NaCl, 10% glycerol, and 1 mM DTT with or without 50 mM glutamine and 50 mM arginine. BCL9 was eluted in 30 mM Tris (pH 7.5), 200 mM NaCl, 50 mM glutamine, 50 mM arginine, and 1 mM DTT. Proteins were aliquoted and stored at −80 °C.

Fluorescence Polarization Assay. FP experiments were performed in Microfluor 2, 96-well, black plates (Thermo Fisher Scientific) and read using a Tecan Ultra plate reader (Tecan U.S. Inc., Research Triangle Park, NC). Saturation experiments for determining the K_d values of fluorescently labeled tracers with β-catenin protein used 50 nM (**1-F**) or 5 nM (**8-F**) tracer and serial dilutions of β-catenin protein (e.g., 1 nM to 10 μM) in assay buffer [100 mM Na_2PO_4 (pH 7.4), 100 μg/mL bovine gamma globulin, and 0.01% Triton X-100 (Invitrogen)] with 4% DMSO to produce a total reaction volume of 125 μL. Competitive FP binding experiments used 50 nM (**1-F**) or 5 nM (**8-F**) tracer, 5 μL of compound in DMSO, and a fixed concentration of β-catenin (typically, 1.5−3 × K_d for the tracer; e.g., K_d = 0.616 μM, β-catenin concentration used = 1.0 μM) in assay buffer to produce a final volume of 125 μL. Dose-dependent experiments were performed in the same manner using no fewer than 10 concentrations of compound diluted by serial dilution. For each assay, negative controls (equivalent to 0% inhibition) contain tracer, β-catenin, and 5 μL of DMSO, while positive controls (equivalent to 100% inhibition) contain only tracer and DMSO in a final volume of 125 μL. Each assay plate was covered with adhesive aluminum foil and gently mixed on an orbital shaker for at least 3 h to reach equilibrium before polarization values were read using excitation and emission wavelengths of 485 and 535 nm, respectively. Percent inhibition was calculated from eq 1

$$\%\text{inhibition} = 100[1 - (\text{mP} - \text{mP}_{\text{free}})/(\text{mP}_{\text{bound}} - \text{mP}_{\text{free}})] \quad (1)$$

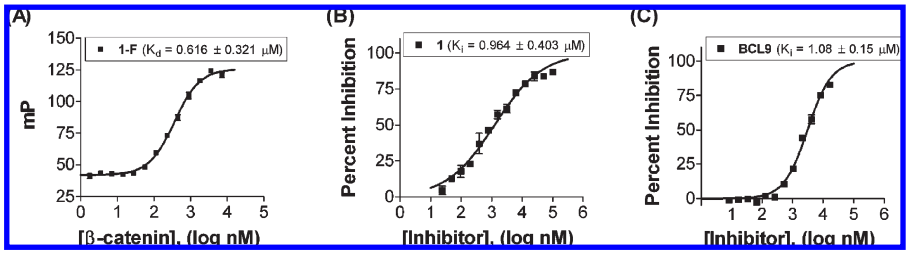

FIGURE 1: (A) Saturation experiment to determine the K_d value for binding of **1-F** to β-catenin. **1-F** (50 nM) was titrated with β-catenin (1−10000 nM) and the FP signal read after 3 h. (B) Competitive binding experiment to determine the ability of unlabeled BCL9 peptide **1** to displace the fluorescently labeled **1-F** (50 nM) from β-catenin (1000 nM). (C) Competitive binding experiment to determine the ability of recombinant BCL9 protein to displace the fluorescently labeled **1-F** (50 nM) from β-catenin (1000 nM). K_i values were calculated from the IC_{50}, K_d, and protein concentration.

where mP_{free} is the signal for the free probe (positive control) and mP_{bound} is the signal for the bound probe (negative control). The IC_{50}, the concentration of inhibitor required to displace 50% of the tracer, was determined by nonlinear least-squares analysis using GraphPad Prism. The K_i values for the compounds were calculated using the equation for FP assays (*34*). Values reported in Table S1 represent the averages and corresponding standard deviations of three or more independent experiments. The Z' factor for the competitive FP assay was calculated as reported previously (*35*).

Surface Plasmon Resonance (SPR) Binding Assays. SPR experiments were performed at room temperature using Biacore 2000 and 3000 optical biosensors. Recombinant BCL9 (residues 347−393) in sodium acetate buffer (pH 5.0) was immobilized at different densities on the Fc2 (4000 response units), Fc3 (2200 response units), and Fc4 (1600 response units) surfaces of a CM-5 sensor chip using standard EDC/NHS coupling chemistry followed by ethanolamine deactivation of the surfaces. The Fc1 surface was used as a control surface and was treated in the same manner as the Fc2 and Fc3 surfaces but in the absence of BCL9.

The binding affinity of recombinant β-catenin (residues 138−686) for immobilized BCL9 was determined by injecting β-catenin solutions with different concentration from 500 to 8000 nM in HBS-EP buffer [10 mM HEPES (pH 7.4), 150 mM NaCl, 3 mM EDTA, and 0.005% (v/v) P20] over the surfaces at a constant flow rate of 20 μL/min. During each injection, the protein or protein complex was allowed to associate or dissociate for 300 or 420 s, respectively. The chip surfaces were regenerated by injecting 50 mM NaOH (2 × 5 μL) followed by washing with the running buffer (2 × 10 μL). The measured response units from the Fc4 surface were normalized by subtracting the signal obtained from the Fc1 control surface. The kinetic and binding parameters, k_{on}, k_{off}, and K_d, were calculated by globally fitting the data to a 1:1 interaction model using BIAEvaluation.

SPR competitive solution binding experiments were performed using a constant concentration of β-catenin protein (300 nM). The protein was preincubated at room temperature for at least 30 min with varying concentrations of synthetic BCL9 peptides. The reaction mixture (20 μL) was injected over the surfaces of the chip at a flow rate of 20 μL/min. Response units were measured at 3 min in the dissociation phase, and the specific binding was calculated by subtracting the signal from the control surface (Fc1) from the surfaces with immobilized BCL9. Percent inhibition was calculated from eq 2,

$$\%\text{inhibition} = 100(1 - \text{RU}/\text{RU}_{\beta\text{-cat}}) \quad (2)$$

where RU is the specific binding signal for β-catenin protein in the presence of the inhibitor and $RU_{\beta\text{-cat}}$ is the specific signal for the β-catenin alone (negative control). For the maximum signal-to-noise ratio, the surface with the highest density of immobilized BCL9 (i.e. Fc2) was used for IC_{50} determinations. IC_{50} values were calculated by nonlinear least-squares analysis using GraphPad Prism 5.0.

RESULTS

Development of an Initial Fluorescence Polarization Assay for the β-Catenin−BCL9 Interaction. Prior studies have demonstrated that the conserved α-helical homology domain 2 (HD2) of BCL9 and B9L is responsible for binding to the first four armadillo (arm) repeats of β-catenin (*6*) with submicromolar affinity (*24*). In addition, the crystal structure of BCL9 complexed with β-catenin and TCF4 (PDB entry 2GL7) reveals that only 19 residues of the BCL9 HD2 region (residues 356−374) have direct contacts with β-catenin (*24*). However, we hypothesized that a BCL9 peptide longer than 19 amino acids may be needed for stabilizing the α-helical secondary structure of the peptide and achieving high binding affinity. For this reason, we first synthesized fluorescein-labeled BCL9 peptide tracer (**1-F**) consisting of 35 residues (residues 347−381). Saturation experiments showed that **1-F** binds to β-catenin with a K_d value of 0.62 ± 0.32 μM (Figure 1A), which is in good agreement with the value previously determined by isothermal calorimetry (*24*).

Using **1-F** as a tracer, we established a competitive FP-based assay. To achieve a reasonable signal-to-noise ratio, we chose to use 1 μM β-catenin and 50 nM **1-F**. To validate the competitive FP assay, we tested the ability of unlabeled BCL9 35-mer peptide **1** and recombinant BCL9 protein to displace **1-F** from β-catenin. Both **1** and BCL9 protein competitively inhibited the binding of **1-F** to β-catenin in a dose-dependent manner, with K_i values of 0.964 ± 0.404 and 1.08 ± 0.15 μM, respectively (Figure 1B, C). Additionally, the B9L peptide **48** was also able to competitively displace **1-F** which was expected on the basis of the high degree of sequence identity in the HD2 regions of BCL9 and B9L (Table S1). These data showed that the binding of **1-F** effectively mimics BCL9 protein binding and the fluorescein tag has no effect on the binding.

Mutational Analysis of Residues Critical for BCL9 Binding to β-Catenin. We next investigated the importance of several key hydrophobic residues in BCL9 for the binding interaction of BCL9 with β-catenin. The crystal structure of BCL9 complexed with β-catenin shows that both basic and hydrophobic residues in BCL9 are involved in binding to β-catenin (*24*). Since the hydrogen bond involving H358 and the salt bridge involving R359 of BCL9 have previously been shown to be critical for binding, and that mutations at these sites abolish binding to β-catenin (*24*, *28*), we did not alter these residues during our mutational studies. Instead, we focused our analysis on L366, I369, L373, and F374, residues that insert into deep hydrophobic pockets in β-catenin (Figure 2A). Mutations at

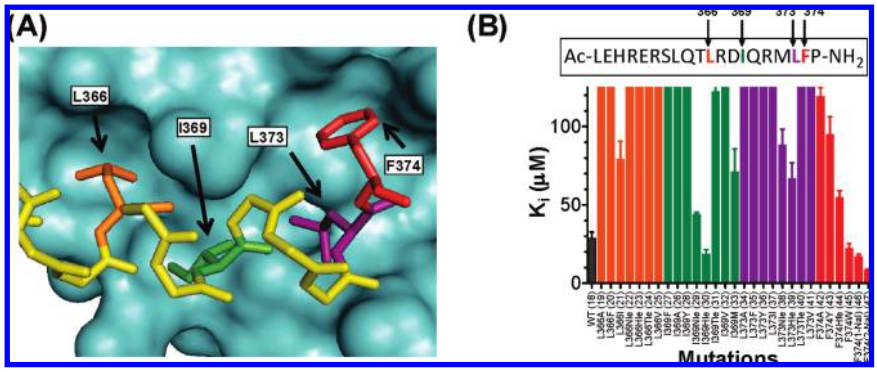

FIGURE 2: (A) Crystal structure of BCL9 in complex with β-catenin (PDB entry 2GL7). β-Catenin is colored cyan. For the sake of clarity, only the side chains of BCL9 residues L366 (orange), I369 (green), L373 (purple), and F374 (red) are shown. The backbones of nonmutated BCL9 residues are colored yellow. (B) K_i values of BCL9 20-mer mutant peptides. Wild-type BCL9 (peptide **18**) is colored black, while single-point mutations for the indicated BCL9 residue are color-coded as in panel A. K_i values were determined using the competitive FP assay with 50 nM **1-F** and 1000 nM β-catenin and are listed in Table S1.

L366, I369, and L373 have previously confirmed the involvement of these residues for binding to β-catenin, but no studies of F374 have been reported. While L373 binds in a deep cleft similar to L366 and I369, F374 binds in a wider and slightly shallower pocket which appeared to be able to accommodate larger ring systems.

To facilitate the synthesis, we employed BCL9 peptides with 20 residues (residues 356−375) spanning those which are visible in the reported β-catenin−BCL9 cocrystal structure (Figure 2A) and have direct contacts with β-catenin. We predicted that, although such shorter peptides may have lower affinities for β-catenin than that of the longer BCL9 35-mer **1** due to a potential decrease in helical propensity, they nevertheless are sufficient for determination of the binding contributions of these residues to β-catenin.

The binding affinities of these mutated BCL9 peptides were then determined using our initial BCL9-competitive FP-based assay. As expected, the wild-type BCL9 20-mer **18** was 30-fold less potent (K_i = 28 μM) than **1** [K_i = 0.964 μM (Table S1)]. Circular dichroism experiments confirmed that the BCL9 35-mer peptide lacking the C-terminal β-Ala-Lys used for labeling (Table S1, peptide **1-b**) was more helical than **18** (16.9% vs 9.7%) in distilled water (data not shown). Using **18** as a standard, we compared the binding affinities of BCL9-based peptides bearing single amino acid mutations at L366, I369, L373, or F374 (Figure 2B and Table S1). As shown in Figure 2B, L366 and L373 were intolerant of substitutions with either larger or smaller hydrophobic residues, with a drastic reduction in binding affinity for all mutant peptides (Table S1, peptides **19**−**25** and **34**−**41**). Most mutations at I369 were also detrimental to binding affinity with the exceptions of norleucine (Nle) and homoleucine (Hle) (Table S1, peptides **29** and **30**), which showed approximately equal binding affinity compared to that of **18**. In contrast, mutation of F374 to residues possessing larger bicyclic aromatic side chains (Table S1, peptides **45**−**47**) resulted in an increase in binding affinity with 2-naphthylalanine (2-Nal) showing the best improvement (3-fold). This result was confirmed in the longer BCL9 35-mer peptide in which the F374(2-Nal) mutation resulted in a similar improvement in binding affinity (Table S1, peptide **2**).

Determination of the Minimal Domain in BCL9 Required for High-Affinity Binding to β-Catenin. Although **18** appeared to possess all of the β-catenin binding residues based upon the BCL9−β-catenin cocrystal structure (PDB entry 2GL7), the longer peptide **1** is 30 times more potent than **18** in its binding affinity for β-catenin. We next determined the minimal domain in BCL9 responsible for its high-affinity binding to β-catenin.

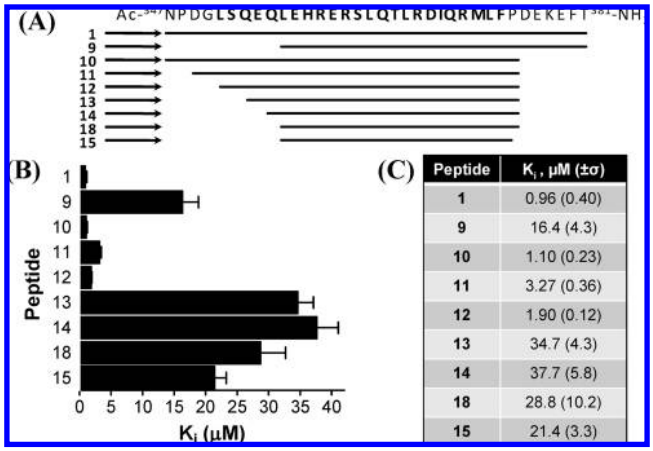

FIGURE 3: (A) BCL9 peptides of different lengths. Peptide sequences correspond to the underlined region. The minimum binding sequence is in bold. (B) BCL9 peptide K_i values determined using a competitive FP-based assay with **1-F** (50 nM) and β-catenin (1000 nM). (C) Table of BCL9 peptide K_i values (averages and standard deviations of three or more experiments).

As shown in Figure 3, removal of the six C-terminal residues of **1** (peptide **10**) did not result in any noticeable decrease in binding affinity. In contrast, deletion of the nine N-terminal residues of **1** (peptide **9**) resulted in a 17-fold decrease in binding affinity for β-catenin.

Having identified the N-terminus of the peptide as being critical to maintaining the wild-type binding affinity of the BCL9 peptide for β-catenin, we proceeded to identify the precise residues which are required for enhancing the binding affinity of BCL9. Since the α-helical region of BCL9 HD2 is predicted to initiate approximately at L351, we systematically deleted two-amino acid sections from the N-terminus of our elongated BCL9 peptide **10**. Evaluation of these increasingly shorter peptides indicated that the four N-terminal amino acids (NPDG) were extraneous, but any further truncation of the peptide resulted in significant (>30-fold) decreases in BCL9 peptide binding affinity (Figure 3B,C, peptides **11**−**14**). These results were in good agreement with a recent report that demonstrated that the L351A mutation in BCL9 protein abolished binding of BCL9 to β-catenin (*28*).

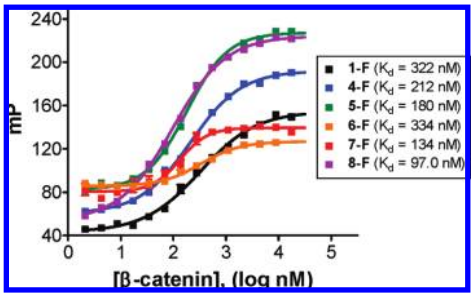

FIGURE 4: Saturation experiments to determine the K_d and dynamic range for shortened BCL9-derived peptide tracers. Each tracer (50 nM for **1-F**, **6-F**, and **7-F** and 5 nM for **4-F**, **5-F**, and **8-F**) was titrated with β-catenin at concentrations ranging from 2 nM to 18 μM in assay buffer containing 0.01% Triton X-100 and 4% DMSO.

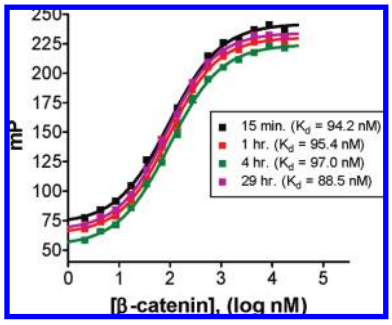

FIGURE 5: Saturation experiment with **8-F** to monitor the K_d and dynamic range over an extended time period. **8-F** (5 nM) was titrated with β-catenin (2 nM to 18 μM) in assay buffer containing 0.01% Triton X-100 and 4% DMSO, and the plate was read at the indicated time points.

Finally, removal of P375 from the C-terminus of **18** had no detrimental effect on the binding of the resulting BCL9 peptide to β-catenin (Figure 3, peptide **15**). Similar results were obtained when P375 was removed from the longer peptide **12** (Table S1, peptide **16**). We concluded from the peptide truncation studies that the minimal domain in BCL9 responsible for its high-affinity binding to β-catenin involves residues 351−374.

Reoptimization of the BCL9-Competitive FP Assay. Having determined the minimal binding sequence of BCL9 required for high-affinity binding to β-catenin and identified certain non-natural amino acids that could further increase the peptide binding affinity, we sought to further optimize the fluorescently labeled tracer used in the FP assay. We synthesized a series of shortened peptide tracers that spanned the minimal binding sequence of BCL9 (residues 351−374) and included the F374(2-Nal) mutation alone or in combination with the I369Hle mutation (Table S1, peptides **3-F**−**8-F**). We also examined the effects of having the fluorescein tag at either the N- or C-terminus, and of using β-alanine or 6-aminohexanoic acid as the spacer between the peptide and the tag.

As shown in Figure 4, attaching fluorescein to the N-terminus of the peptide (peptides **6-F** and **7-F**) resulted in a narrow dynamic range of ~70 mP, whereas labeling on the C-terminus gave an excellent dynamic range of more than 160 mP (**4-F**, **5-F**, and **8-F**). Furthermore, relatively high concentrations (50 nM) of N-terminally labeled peptides were required to achieve adequate fluorescence signal, while C-terminally labeled tracers gave an excellent fluorescence signal at concentrations as low as 5 nM (data not shown).

Inclusion of the I369Hle mutation in addition to the F374-(2-Nal) mutation (peptides **3-F**−**6-F**) resulted in no additional enhancement in binding affinity as compared to peptides with only the F374(2-Nal) mutation [peptides **7-F** and **8-F** (Figure 4)]. In comparing the type of linker used to attach fluorescein, we found that the two-β-alanine spacer on the C-terminus of the peptide to link the lysine(FAM) conjugate was slightly better than the 6-aminohexanoic acid spacer (data not shown). We therefore chose **8-F** as the optimized tracer for the FP assay.

Saturation experiments showed that **8-F** has a K_d value of 101 ± 42 nM for binding to β-catenin. Furthermore, the FP signal and K_d were stable over 29 h (Figure 5) and were not affected by 4% DMSO (Figure S1 of the Supporting Information). For the purpose of high-throughput screening, we tested the effect of the surfactant Triton X-100, which can minimize aggregation effects by hydrophobic molecules. Our data showed that 0.01% of the Triton X-100 had no significant effect on the FP signal or K_d, but higher concentrations (0.05 and 0.1%) caused a decrease in K_d and the assay dynamic range (Figure S2 of the Supporting Information).

In reoptimizing our competitive FP assay, we selected concentrations of 250 nM β-catenin and 5 nM **8-F**. Similar to the results from the saturation experiments, the optimized competitive assay with **8-F** demonstrated a marked improvement in the assay dynamic range (84 mP) compared to the original assay with **1-F** (dynamic range of 49 mP). To assess the quality of our reoptimized assay for use as a high-throughput screening assay, we calculated the statistical parameter Z' which reflects the dynamic range of the assay as well as the deviation in the controls (*35*). High-quality assays should have Z'-factors nearing the maximum value of 1, with a typical cutoff value for acceptable HTS assays of 0.5. As shown in Figure 6, the reoptimized competitive FP assay has a Z' of 0.72 compared to a Z' of 0.29 for the original assay using **1-F**, thus indicating the suitability of our optimized FP assay for HTS purposes.

Development of a SPR-Based Binding Assay. FP assays have several advantages that make them desirable as HTS assays. These include simplicity, homogeneous reactions, and relatively cheap operating costs. However, being a fluorescence-based technique, an FP assay can be affected by compounds that have absorption or emission spectra overlapping with those of the fluorescent probe. To address this issue, we developed a complementary SPR-based secondary assay designed to eliminate false positive hits from our FP assay resulting from autofluorescent compounds. Since SPR-based assays are based on biophysical principles independent of those involved in fluorescence-based techniques, they are not affected by autofluorescence (*36*).

For our SPR-based assay, we immobilized recombinant BCL9 protein on the surface of the SPR sensor chip using standard EDC/NHS amide coupling chemistry. BCL9 protein was immobilized at different densities on the Fc2 (4000 response units), Fc3 (2200 response units), and Fc4 (1600 response units) surfaces of the chip, while the Fc1 surface was used as a control surface to account for nonspecific binding to the chip.

We evaluated the binding of recombinant β-catenin to immobilized BCL9 using several different concentrations of β-catenin ranging from 500 nM to 8 μM and determined that β-catenin binds to immobilized BCL9 with a K_d value of 2.9 μM (Figure 7). This value is in good agreement with the binding affinity of the BCL9 peptide in our FP assay [K_i = 1.1 μM (Figure 1)], suggesting that immobilized and free BCL9 proteins interact with β-catenin very similarly.

To validate the SPR assay, we tested if our synthetic BCL9 peptides can disrupt the binding of β-catenin to immobilized

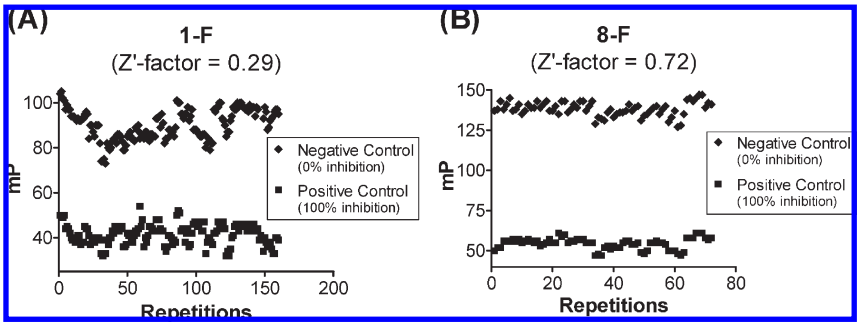

FIGURE 6: Calculated Z'-factors for competitive FP-based assays using **1-F** and **8-F**. (A) Original competitive FP-based assay using **1-F** (50 nM) and β-catenin (1 μM). (B) Reoptimized competitive FP-based assay using **8-F** (5 nM) and β-catenin (250 nM). Positive controls representing 100% inhibition contain only tracer. Negative controls representing 0% inhibition contain tracer and β-catenin. Points represent the control wells from experiments performed in separate 96-well plates.

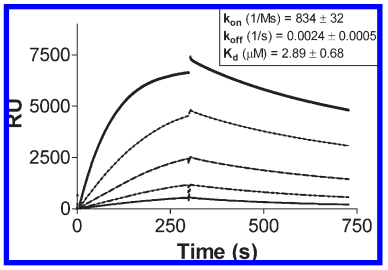

FIGURE 7: Determination of kinetic and steady state parameters for β-catenin binding to immobilized BCL9 protein. The sensorgrams indicate the responses when varying concentrations (from bottom to top, 0.5, 1, 2, 4, and 8 μM) of β-catenin were injected over immobilized BCL9. k_{on}, k_{off}, and K_d were calculated by simultaneous nonlinear regression.

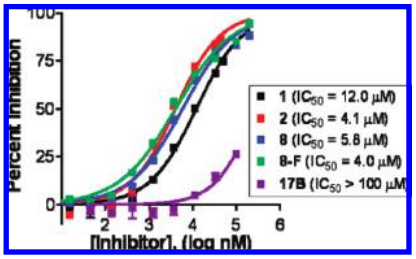

FIGURE 8: Competitive binding experiment for determining the ability of synthetic BCL9 peptides to inhibit the binding of β-catenin to BCL9 protein. β-Catenin (300 nM) was preincubated with varying concentrations of peptide inhibitors for at least 30 min, and then 20 μL of the reaction mixture was injected at a rate of 20 μL/min over the immobilized BCL9. IC_{50} values were determined by nonlinear least-squares analysis.

BCL9 protein. β-Catenin protein was preincubated with varying concentrations of synthetic BCL9 peptides and then injected over the surface of the chip. As shown in Figure 8, the wild-type BCL9 35-mer (**1**) inhibits the binding of β-catenin to BCL9 with an IC_{50} value of 12 μM, which is in reasonable agreement with the determined IC_{50} of 3.5 μM (K_i = 0.96 μM) from our FP experiments. Furthermore, peptides bearing the 2-naphthylalanine substitution at F374 (**2**, **8**, and **8-F**) exhibit the same 2−3-fold enhancement in binding affinity, consistent with the data obtained in our FP experiment. The specificity of our competitive SPR-based assay was confirmed using peptide **17B** as a negative control. This peptide, which contains known inactivating alanine mutations at residues L366 and I369 (*24*) and which is inactive in our FP assay (Table S1), was likewise found to be more than 10-fold less potent than wild-type peptide **1** in our competitive SPR-based assay. Thus, our competitive SPR-based assay can quantitatively determine the binding affinities of BCL9 peptides for β-catenin in competition with the recombinant BCL9 protein, and the results are consistent with those obtained using our FP assay. Therefore, this SPR assay can serve as a useful secondary assay with which to confirm the inhibition of binding of BCL9 to β-catenin by compounds identified in our FP-based HTS assay.

DISCUSSION

The canonical Wnt signaling pathway regulates numerous cellular processes such as cell proliferation, differentiation, and survival. β-Catenin is the primary mediator of the canonical Wnt signaling pathway, and its expression is strictly controlled in normal cells. However, in cancer, β-catenin is frequently upregulated, which contributes to tumorigenesis (*2*, *3*, *37*).

The transcriptional activation of β-catenin has been shown to be dependent upon the formation of a nuclear supercomplex comprised of β-catenin and various cofactors, including TCF/LEF, BCL9/B9L, and CBP (*6*, *13*, *30*, *38*−*40*). Disruption of this complex has been proposed as a new cancer therapeutic strategy. Recently, several studies have demonstrated the feasibility of this approach. Indeed, several nonpeptide small molecules have been identified that inhibit the binding of β-catenin to TCF/LEF or CBP (*17*, *18*, *27*). Some of these compounds were also shown to inhibit β-catenin-mediated transcriptional activation, downregulate Wnt-targeted gene expression, inhibit cell proliferation, and induce apoptosis in cancer cells with constitutively activated β-catenin (*17*, *19*, *27*). However, rigorous biophysical analysis and characterization *in vivo* still need to be completed for these compounds. Furthermore, because of the overlapping binding sites of TCF/LEF, E-cadherin, APC, and Axin, it may ultimately prove to be challenging to develop selective inhibitors of the binding interaction of TCF/LEF with β-catenin without interfering with the interactions of β-catenin and its other binding partners. Indeed, a number of reported TCF inhibitors were also shown to disrupt the binding of β-catenin to APC.

BCL9 and B9L, on the other hand, primarily bind to a unique binding site located in the N-terminal armadillo (arm) repeat of β-catenin. Analysis of the crystal structure of β-catenin in complex with BCL9 and TCF indicates that the α-helical HD2 region of BCL9 binds in a well-defined groove in the first arm repeat of β-catenin and does not make any observable contacts with TCF or its binding site on β-catenin (*24*). Therefore, inhibitors that bind at the BCL9 binding site may have little or no effect on the interactions of β-catenin with its cytosolic binding partners (*24*, *28*). Despite this key advantage over

targeting TCF, no inhibitors of the interaction of BCL9 with β-catenin have been reported. This could be, in part, due to the relatively recent discovery of BCL9 as a required component of the β-catenin transcriptional activation complex in human cells. Recently, BCL9 was shown to specifically enhance β-catenin-mediated transcriptional activation in lymphoid cells (*29*). BCL9 and its closely related partner, B9L, were also shown to be crucial to the activity of β-catenin in SW480 colon cancer cells with constitutively activated β-catenin and in Wnt3A-stimulated HEK 293 cells (*28*). Additionally, siRNA knockdown of B9L was shown to reduce the level of cell migration, induce an epithelial-like phenotype, and inhibit colony formation in colon cancer cell lines (*32*). These studies have thus suggested that blocking the BCL9−β-catenin interaction using small-molecule inhibitors represents an attractive cancer therapeutic strategy.

With respect to the discovery of small-molecule inhibitors of the BCL9−β-catenin interaction, we have developed two quantitative and complementary BCL9-specific binding assays. We have first developed a FP-based binding assay employing a fluorescently labeled 35-residue BCL9 peptide (**1-F**) and recombinant β-catenin protein and determined that they have a K_d value of 616 nM. This first competitive FP assay, however, had a narrow dynamic range (~45 mP) and a calculated Z'-factor of 0.29, making it unsuitable as an HTS assay. We therefore performed extensive mutational analysis on four critical binding residues (L366, I369, L373, and F374) and showed that while the first three sites were intolerant to mutation, the substitution of 2-naphthylalanine at F374 could increase the binding affinity of the peptide by 3-fold. We also sought to reduce the overall length of our tracer and subsequently mapped the minimal binding sequence of BCL9 to residues 351−374. Our minimal binding sequence is consistent with the recent report by de la Roche *et al.* (*28*), which demonstrated that L351, despite being distant from the β-catenin binding pocket, was critical for the binding of BCL9. Using the results of our peptide mapping and mutation experiments, we were able to develop an optimized tracer (**8-F**) that is nine residues shorter than **1-F** and had a K_d value of 101 nM. This led to an optimized FP-based competitive assay using **8-F**, which has a large dynamic range, an excellent signal-to-noise ration, and a calculated Z'-factor to 0.72, making this assay suitable for HTS.

Also noteworthy was the fact that our optimized FP assay utilized a more stable preparation of purified recombinant β-catenin. During our original experiments, we found that the β-catenin protein was unstable and tended to precipitate after being stored for 1−2 months at −80 °C, even in the presence of 10% glycerol. This was a contributing factor to the higher than normal standard deviations in our initial assays (Figure 6). To address this issue, we found that adding 50 mM glutamine and 50 mM arginine to the buffer helped stabilize the protein, giving higher yields of soluble protein that did not show signs of precipitation after being stored for more than 6 months. Using this more stable preparation of β-catenin, we also found that the K_d and K_i values of our peptides were on average twice as potent (compare **1-F** from Figures 1A and 4); however, the same trends in potencies for mutated peptides and wild-type peptides of varying lengths remained unchanged.

Since fluorescence-based FP assays are prone to having false positive results due to autofluorescent compounds, we also developed an SPR-based binding assay to complement our FP assay. SPR-based techniques, which are not reliant on molecular fluorescence, are useful for discriminating between compounds that truly inhibit protein−protein binding and eliminate false positives arising from compounds that absorb light or fluoresce at wavelengths similar to those of the fluorescent probe in the FP assay. For our SPR-based assay, we immobilized recombinant BCL9 protein (residues 347−393) and demonstrated that it binds to β-catenin with a K_d value of 2.9 μM. This value was in good agreement with the K_i value of 1.1 μM for the recombinant BCL9 protein determined in our FP assay and suggested that the immobilized BCL9 protein binds to β-catenin in a manner similar to that of the recombinant BCL9 protein in solution.

We next developed and optimized the conditions for a competitive SPR assay. Using our BCL9-derived peptides, we showed that BCL9 peptides effectively inhibit the binding of β-catenin to the immobilized BCL9 protein in a dose-dependent manner, and the determined IC_{50} values in the SPR assay are in good agreement with those measured in our FP assay.

In summary, we have developed an optimized FP-based binding assay for the BCL9−β-catenin interaction. We have demonstrated that this simple and quantitative FP assay is suitable for adaptation to HTS. We have also developed and validated a complementary SPR-based secondary binding assay. Our extensive mutational and truncation analysis on the BCL9 binding domain provided further insights into the interaction between BCL9 and β-catenin. The establishment of two complementary, quantitative, and reliable biochemical binding assays has laid the foundation for the design and discovery of potent and specific small-molecule inhibitors of the BCL9−β-catenin interaction.

ACKNOWLEDGMENT

We thank Dr. Jason Gestwicki of the Department of Pathology and Life Sciences Institute at the University of Michigan for the use of his Biacore 3000 optical biosensor and Dr. Ari Gafni of the Biophysics Research Division at the University of Michigan for the use of his circular dichroism spectrophotometer. The β-catenin cDNA was a kind gift from Dr. Wenqing Xu of the Department of Biological Structure at the University of Washington. The BCL9 cDNA was kindly provided by Dr. Konrad Basler of the Institut für Molekularbiologie at the Universität Zürich.

SUPPORTING INFORMATION AVAILABLE

A complete listing of peptide sequences, characterization and binding affinities, and FP assay DMSO and Triton X-100 experiments. This material is available free of charge via the Internet at http://pubs.acs.org.

REFERENCES

1. Morin, P. J. (1999) β-Catenin signaling and cancer. *BioEssays 21*, 1021–1030.
2. Bienz, M., and Clevers, H. (2000) Linking colorectal cancer to Wnt signaling. *Cell 103*, 311–320.
3. Polakis, P. (2000) Wnt signaling and cancer. *Genes Dev. 14*, 1837–1851.
4. Hoffmans, R., and Basler, K. (2004) Identification and in vivo role of the Armadillo-Legless interaction. *Development 131*, 4393–4400.
5. Hoffmans, R., Städeli, R., and Basler, K. (2005) Pygopus and legless provide essential transcriptional coactivator functions to Armadillo/β-catenin. *Curr. Biol. 15*, 1207–1211.
6. Kramps, T., Peter, O., Brunner, E., Nellen, D., Froesch, B., Chatterjee, S., Murone, M., Zullig, S., and Basler, K. (2002) Wnt/wingless signaling requires BCL9/legless-mediated recruitment of pygopus to the nuclear β-catenin-TCF complex. *Cell 109*, 47–60.
7. Mosimann, C., Hausmann, G., and Basler, K. (2006) Parafibromin/hyrax activates Wnt/Wg target gene transcription by direct association with β-catenin/armadillo. *Cell 125*, 327–341.

8. Städeli, R., and Basler, K. (2005) Dissecting nuclear Wingless signalling: Recruitment of the transcriptional co-activator Pygopus by a chain of adaptor proteins. *Mech. Dev. 122*, 1171–1182.
9. He, T. C., Sparks, A. B., Rago, C., Hermeking, H., Zawel, L., da Costa, L. T., Morin, P. J., Vogelstein, B., and Kinzler, K. W. (1998) Identification of c-MYC as a target of the APC pathway. *Science 281*, 1509–1512.
10. Kim, P. J., Plescia, J., Clevers, H., Fearon, E. R., and Altieri, D. C. (2003) Survivin and molecular pathogenesis of colorectal cancer. *Lancet 362*, 205–209.
11. Leung, J. Y., Kolligs, F. T., Wu, R., Zhai, Y. L., Kuick, R., Hanash, S., Cho, K. R., and Fearon, E. R. (2002) Activation of AXIN2 expression by β-catenin-T cell factor: A feedback repressor pathway regulating Wnt signaling. *J. Biol. Chem. 277*, 21657–21665.
12. Tetsu, O., and McCormick, F. (1999) β-Catenin regulates expression of cyclin D1 in colon carcinoma cells. *Nature 398*, 422–426.
13. Yamada, T., Takaoka, A. S., Naishiro, Y., Hayashi, R., Maruyama, K., Maesawa, C., Ochiai, A., and Hirohashi, S. (2000) Transactivation of the Multidrug Resistance 1 gene by T-cell factor 4/β-catenin complex in early colorectal carcinogenesis. *Cancer Res. 60*, 4761–4766.
14. Janssens, N., Janicot, M., and Perera, T. (2006) The Wnt-dependent signaling pathways as target in oncology drug discovery. *Invest. New Drugs 24*, 263–280.
15. Takahashi-Yanaga, F., and Sasaguri, T. (2007) The Wnt/β-catenin signaling pathway as a target in drug discovery. *J. Pharmacol. Sci. (Tokyo, Jpn.) 104*, 293–302.
16. Takemaru, K. I., Ohmitsu, M., and Li, F. Q. (2008) An oncogenic hub: β-Catenin as a molecular target for cancer therapeutics. *Handb. Exp. Pharmacol.,* 261–284.
17. Lepourcelet, M., Chen, Y. N. P., France, D. S., Wang, H. S., Crews, P., Petersen, F., Bruseo, C., Wood, A. W., and Shivdasani, R. A. (2004) Small-molecule antagonists of the oncogenic Tcf/β-catenin protein complex. *Cancer Cell 5*, 91–102.
18. Trosset, J. Y., Dalvit, C., Knapp, S., Fasolini, M., Veronesi, M., Mantegani, S., Gianellini, L. M., Catana, C., Sundstrom, M., Stouten, P. F., and Moll, J. K. (2006) Inhibition of protein-protein interactions: The discovery of druglike β-catenin inhibitors by combining virtual and biophysical screening. *Proteins 64*, 60–67.
19. Minke, K. S., Staib, P., Puetter, A., Gehrke, I., Gandhirajan, R. K., Schlosser, A., Schmitt, E. K., Hallek, M., and Kreuzer, K. A. (2009) Small molecule inhibitors of WNT signaling effectively induce apoptosis in acute myeloid leukemia cells. *Eur. J. Haematol. 82*, 165–175.
20. Gottardi, C. J., and Gumbiner, B. M. (2004) Distinct molecular forms of β-catenin are targeted to adhesive or transcriptional complexes. *J. Cell Biol. 167*, 339–349.
21. Graham, T. A., Weaver, C., Mao, F., Kimelman, D., and Xu, W. Q. (2000) Crystal structure of a β-catenin/Tcf complex. *Cell 103*, 885–896.
22. Huber, A. H., Nelson, W. J., and Weis, W. I. (1997) Three-dimensional structure of the armadillo repeat region of β-catenin. *Cell 90*, 871–882.
23. Huber, A. H., and Weis, W. I. (2001) The structure of the β-catenin/E-cadherin complex and the molecular basis of diverse ligand recognition by β-catenin. *Cell 105*, 391–402.
24. Sampietro, J., Dahlberg, C. L., Cho, U. S., Hinds, T. R., Kimelman, D., and Xu, W. Q. (2006) Crystal structure of a β-catenin/BCL9/Tcf4 complex. *Mol. Cell 24*, 293–300.
25. Stappert, J., and Kemler, R. (1994) A Short Core Region of E-Cadherin Is Essential for Catenin Binding and Is Highly Phosphorylated. *Cell Adhes. Commun. 2*, 319–327.
26. Perl, A. K., Wilgenbus, P., Dahl, U., Semb, H., and Christofori, G. (1998) A causal role for E-cadherin in the transition from adenoma to carcinoma. *Nature 392*, 190–193.
27. Emami, K. H., Nguyen, C., Ma, H., Kim, D. H., Jeong, K. W., Eguchi, M., Moon, R. T., Teo, J. L., Oh, S. W., Kim, H. Y., Moon, S. H., Ha, J. R., and Kahn, M. (2004) A small molecule inhibitor of β-catenin/cyclic AMP response element-binding protein transcription. *Proc. Natl. Acad. Sci. U.S.A. 101*, 12682–12687.
28. de la Roche, M., Worm, J., and Bienz, M. (2008) The function of BCL9 in Wnt/β-catenin signaling and colorectal cancer. *BMC Cancer,* 8.
29. Sustmann, C., Flach, H., Ebert, H., Eastman, Q., and Grosschedl, R. (2008) Cell-type-specific function of BCL9 involves a transcriptional activation domain that synergizes with β-catenin. *Mol. Cell. Biol. 28*, 3526–3537.
30. Thompson, B. J. (2004) A complex of armadillo, legless, and pygopus coactivates dTCF to activate wingless target genes. *Curr. Biol. 14*, 458–466.
31. Adachi, S., Jigami, T., Yasui, T., Nakano, T., Ohwada, S., Omori, Y., Sugano, S., Ohkawara, B., Shibuya, H., Nakamura, T., and Akiyama, T. (2004) Role of a BCL9-related β-catenin-binding protein, B9L, in tumorigenesis induced by aberrant activation of Wnt signaling. *Cancer Res. 64*, 8496–8501.
32. Brembeck, F. H., Schwarz-Romond, T., Bakkers, J., Wilhelm, S., Hammerschmidt, M., and Birchmeier, W. (2004) Essential role of BCL9-2 in the switch between β-catenin's adhesive and transcriptional functions. *Genes Dev. 18*, 2225–2230.
33. Kaiser, E., Colescot, R. L., Bossinge, C. D., and Cook, P. I. (1970) Color Test for Detection of Free Terminal Amino Groups in Solid-Phase Synthesis of Peptides. *Anal. Biochem. 34*, 595–598.
34. Nikolovska-Coleska, Z., Wang, R. X., Fang, X. L., Pan, H. G., Tomita, Y., Li, P., Roller, P. P., Krajewski, K., Saito, N. G., Stuckey, J. A., and Wang, S. M. (2004) Development and optimization of a binding assay for the XIAP BIR3 domain using fluorescence polarization. *Anal. Biochem. 332*, 261–273.
35. Zhang, J. H., Chung, T. D. Y., and Oldenburg, K. R. (1999) A simple statistical parameter for use in evaluation and validation of high throughput screening assays. *J. Biomol. Screening 4*, 67–73.
36. Fägerstam, L. G., Frostell-Karlsson, Å., Karlsson, R., Persson, B., and Rönnberg, I. (1992) Biospecific interaction analysis using surface plasmon resonance detection applied to kinetic, binding site and concentration analysis. *J. Chromatogr. 597*, 397–410.
37. Clevers, H. (2006) Wnt/β-catenin signaling in development and disease. *Cell 127*, 469–480.
38. Hecht, A., Vleminckx, K., Stemmler, M. P., van Roy, F., and Kemler, R. (2000) The p300/CBP acetyltransferases function as transcriptional coactivators of β-catenin in vertebrates. *EMBO J. 19*, 1839–1850.
39. Hsu, S. C., Galceran, J., and Grosschedl, R. (1998) Modulation of transcriptional regulation by LEF-1 in response to Wnt-1 signaling and association with β-catenin. *Mol. Cell. Biol. 18*, 4807–4818.
40. Takemaru, K. I., and Moon, R. T. (2000) The transcriptional coactivator CBP interacts with β-catenin to activate gene expression. *J. Cell Biol. 149*, 249–254.